International Journal of Biological Macromolecules 233 (2023) 123530

Contents lists available at ScienceDirect

International Journal of Biological Macromolecules

journal homepage: www.elsevier.com/locate/ijbiomac

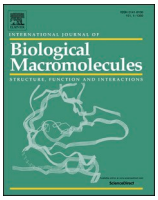

Design and assembly of biodegradable capsules based on alginate hydrogel composite for the encapsulation of blue dye

Yasmin Kabalan [a], Xavier Montané [b,*], Bartosz Tylkowski [c], Silvia De la Flor [d], Marta Giamberini [a]

[a] Department of Chemical Engineering, Universitat Rovira i Virgili, Av. Països Catalans 26, Campus Sescelades, 43007 Tarragona, Spain
[b] Department of Analytical Chemistry and Organic Chemistry, Universitat Rovira i Virgili, C/Marcel·lí Domingo 1, 43007 Tarragona, Spain
[c] Eurecat, Centre Tecnològic de la Química de Catalunya, C/Marcel·lí Domingo s/n, 43007 Tarragona, Spain
[d] Department of Mechanical Engineering, Universitat Rovira i Virgili, Av. Països Catalans 26, Campus Sescelades, 43007 Tarragona, Spain

ARTICLE INFO

Keywords:
Biodegradable capsules
Alginate
Blue dye

ABSTRACT

The encapsulation of bluing agents in biodegradable polymeric capsules is an emerging option in laundry detergents sector to substitute formaldehyde-based polymers, because they are non-biodegradable, carcinogenic and toxic. In this work, we present for the first time the successful encapsulation of a blue dye in biodegradable capsules which shell was formed by an alginate hydrogel and a polyethylene glycol network. Different types of capsules were synthesized (addition or not of the diacrylate monomer) and irradiation of the crosslinking solution at different times. Furthermore, a deep characterization of each type of capsules was performed (chemical and morphological characterization, assessment of their mechanical and thermal properties, evaluation of their biodegradability), noting that the incorporation of the diacrylate monomer (PEGDMA) and the two different irradiation times selected substantially affected the final properties of the capsules. The obtained results will serve to comprehend how the dye can be released from the capsules.

1. Introduction

Encapsulation, which consists in the entrapment of a material into the core of an empty particle, called capsule, has been utilized in many sectors (food, pharmaceutical, paper and textile industry, cosmetics, agrochemicals, personal care, household care, etc.) mainly to prevent the degradation of the active compounds from the media and favor the controlled release of the encapsulated compound [1–3]. For instance, the encapsulation of food additives masks some undesired flavors [4] while drugs are encapsulated to control their release and target tumor sites [5]. As far as the agricultural sector is concerned, the use of encapsulation can help to reduce the quantity of pesticides that should be applied, thus reducing their environmental impact [6].

Another sector in which the developed encapsulation technologies are currently being used more and more is the laundry detergents, which are essential commodities that are used all over the world. As evidence of this fact, the global market for laundry detergents was $152.4 billion in 2020 and is expected to grow at an annual rate of around 5.0 % from 2021 to 2028 to overpass $223.8 billion in 2028 [7]. Currently, the encapsulation of fragrances in laundry detergent industry preserves perfumes from the detergent media and permit their controlled release during or even after the washing process.

Moreover, the encapsulation of bleaching agents (inorganic compounds such as hypochlorites, chlorines, peroxides, etc. or organic compounds that absorb light in the UV region like the bluing agent or fluorescent whitening agents (FWA)) is an emerging alternative that can be explored to restore the whiteness of clothes and to diminish the yellowing of the white-colored clothes, fibers or other textile materials and their damage over time [8,9].

Generally, the shell of these type of capsules is made of a polymeric material [10,11]. Nonetheless, formaldehyde-based shells (urea-formaldehyde and melamine-formaldehyde) are the only ones that can endure the detergent's aggressive media [12–14], despite the many drawbacks of formaldehyde derived materials, since formaldehyde is a carcinogenic, toxic and non-biodegradable material [15–17]. Additionally, the fragmentation of these non-biodegradable plastic capsules when they are released into the environment after their usage, leads to the formation of microplastics, which are responsible for the pollution of

* Corresponding author.
E-mail address: xavier.montane@urv.cat (X. Montané).

https://doi.org/10.1016/j.ijbiomac.2023.123530
Received 15 July 2022; Received in revised form 20 January 2023; Accepted 30 January 2023
Available online 3 February 2023

rivers, lakes, and oceans [18,19]. Furthermore, some studies suggest that the accumulation of microplastics, once ingested by animals, can be associated to some diseases [20].

Therefore, one attractive option that can be explored to improve the stability of the capsules shell based on more sustainable materials, consists of the preparation of multicomponent shell capsules with biodegradable materials.

Recently, one biocompatible compound that has been highly employed in the encapsulation technologies is alginate. Alginates are natural polysaccharides which consist of a linear chain of (1–4) linked residues of α-L-guluronate (G) and β-D-mannuronate (M) in different proportions and sequential arrangements (Fig. 1a) [21]. Alginates are found in brown algae and are extensively used in microencapsulation due to their high versatility and biocompatibility offered when they gel in presence of divalent ions such as Ca^{2+} to give rise to a cross-linked complex (Fig. 1b) [22,23]. On the other hand, poly(ethylene glycol) (PEG) monomers can be chemically modified using simple methods to facilitate their crosslinking, such as acrylic functionalization, and thus employed in the formation of biocompatible capsules through free radical polymerization (Fig. 1c and d) [24,25].

In this sense, the novelty of this study has been to report for the first time the encapsulation of a dye used in laundry detergent industry in potentially biodegradable macrocapsules formed by a multilayer shell: the first shell is constituted by alginate, which in turn is coated by a second shell based on poly(ethylene glycol) dimethacrylate (PEGDMA), with the aim to hold the dye stable in the detergent media and let its release after the mechanical breakage of the capsules in the washing machine (Fig. 1e). As a matter of fact, we explored this approach in the macro-scale because this allowed an easier characterization of these complex systems, which is the purpose of this investigation.

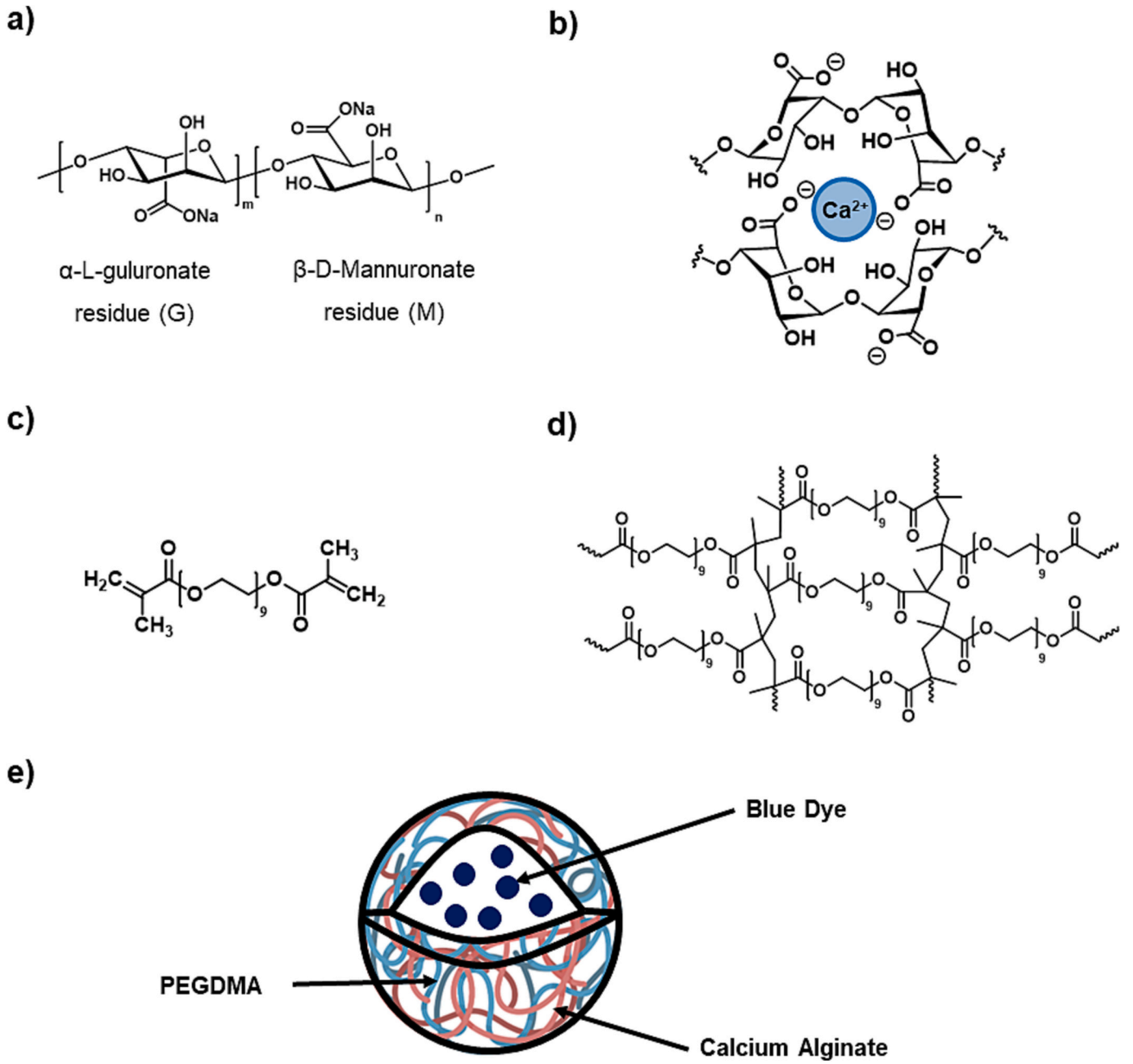

Fig. 1. Chemical structure of: a) sodium alginate; b) Crosslinking of alginate chains by calcium ions; c) Poly(ethyleneglycol) 400 dimethacrylate (PEGDMA); d) Crosslinked PEGDMA; and e) general scheme of the synthesized capsules with the encapsulated blue dye.

To accomplish this objective, we take advantage of a simple extrusion process to control the polymerization of both monomers: the gelation of sodium alginate and the UV polymerization of PEGDMA monomer. Various aspects of this method were studied to obtain a greater control of the process and manage to synthesize optimal capsules for the desired application: the type of acrylate monomer and the dye used, the encapsulation of different concentrations of the dye, the time at which the samples were irradiated, etc.

The obtained macrocapsules were thoroughly characterized concerning their chemical, morphological, mechanical and thermal properties as well as their biodegradability in water. This complete characterization study also aims at understanding the possible rupture mechanisms of the capsules and thus realize how the encapsulated dye is released.

2. Materials and methods

2.1. Materials

Sodium alginate (Viscosity (1 % in water; 20 °C): 350–550 mPa·s; MW: 10,000–600,000 g/mol) was purchased from Panreac ITW Reagents (Panreac Química SLU, Castellar del Vallès, Spain). Calcium chloride (≥97 %) was purchased from Honeywell International Inc. (Charlotte, NC, USA). Auramine O Dye (Dye content >80 %) and Reactive orange 16 (Dye content >70 %) were purchased from Sigma-Aldrich (Sigma Aldrich, Burlington, MA, USA), while Active Violet Ion (AVI) was provided by Procter & Gamble (Cincinnati, OH, USA). Poly (ethylene glycol) diacrylate (PEGDA, average $M_n \approx 250$ g/mol), Irgacure 1173 (2-hydroxy-2-methylpropiphenone (97 %)) and Alkaline buffer solution (1.5 M, pH = 10.3, (25 °C)) were purchased from Sigma Aldrich (Sigma Aldrich, Burlington, MA, USA). Poly(ethyleneglycol) 400 dimethacrylate (PEGDMA, average $M_n \approx 600$ g/mol) was purchased from SARTOMER (Exton, PA, USA). Sodium hydroxide (ACS reagent, ≥98.5 %, pellets, for synthesis) was purchased from Scharlau (Scharlab S. L., Sentmenat, Barcelona, Spain), while hydrochloric acid (37 %) was purchased from Fisher Scientific (Madrid, Spain). All the chemical compounds were used as provided without any further purification.

2.2. Preparation of the macrocapsules

For the synthesis of the capsules, different steps were performed:

- First, a solution of 100 mL of water that contained 1 % *w*/w sodium alginate (and the corresponding dye, the acrylate monomer and a radical initiator according to the different formulations presented in Table 1) was prepared. Once the solution was completely homogeneous, it was then extruded through a syringe-needle system dropwise into a crosslinking solution (250 mL of water containing 2 % *w*/w calcium chloride). To favor the extrusion, a pump that works at a flowrate of 1 mL/min was used, while the distance between the needle and the crosslinking solution was fixed at 5.5 cm.
- If an acrylate derived monomer was added to build up the shell of the capsules (PEGDA or PEGDMA), the polymerization of these samples was carried out using an UV curing lamp from Helios Italquartz. Precisely, the exposure was done for 5 min using 50 % power at 7.5 A. Regarding the irradiation procedure, some samples were irradiated directly after being extruded into the crosslinking solution and then they were left under stirring for 24 h, while the other samples were irradiated after being stirred for 24 h. In all the cases, the irradiation time was 5 min.
- At this point, the capsules were filtered, dried in an oven at 40 °C for 24 h before examining their properties.

Table 1
Composition of the prepared capsules.

Sample	Sodium alginate (% *w*/w respect to the polymeric solution)	PEGDA (% w/w respect to the polymeric solution)	PEGDMA (% w/w respect to the polymeric solution)	Photoinitiator (Irgacure 1173) (% w/w respect to acrylate monomer)	Dye	Dye Amount (% w/w respect to the polymeric solution)	Time before UV irradiation (h)[a]
A	1	–	–	–	–	–	–
A-RO1	1	–	–	–	Reactive Orange 16	1	–
A-RO0.1	1	–	–	–	Reactive Orange 16	0.1	–
A-RO0.2	1	–	–	–	Reactive Orange 16	0.2	–
A-RO0.3	1	–	–	–	Reactive Orange 16	0.3	–
A-AO0.03	1	–	–	–	Auramine O	0.03	–
A-AVI0.1	1	–	–	–	AVI	0.1	–
A-AVI0.3	1	–	–	–	AVI	0.3	–
A-AVI0.5	1	–	–	–	AVI	0.5	–
A-AVI0.8	1	–	–	–	AVI	0.8	–
A-AVI0.8 -UV0h	1	–	–	–	AVI	0.8	0
A-P-AVI0.8-UV0h	1	1	–	5	AVI	0.8	0
A-P-AVI0.8-UV24h	1	1	–	5	AVI	0.8	24
A-PM-UV0h	1	–	1	5	–	–	0
A-PM-UV24h	1	–	1	5	–	–	24
A-PM-AVI0.8-UV0h	1	–	1	5	AVI	0.8	0
A-PM-AVI0.8-UV24h	1	–	1	5	AVI	0.8	24

[a] At time = 0, the samples were irradiated just after the extrusion of the polymeric solution into the crosslinking solution, while at time = 24 h, the samples were irradiated after being stirred for 24 h together with the crosslinking solution.

The overall process followed is depicted in Fig. 2 and the chemical composition of all the samples is summarized in Table 1.

2.3. Characterization techniques

2.3.1. Fourier-transform infrared spectroscopy (FTIR)

The FTIR spectra of selected samples were recorded on a Vertex 70 FTIR spectrophotometer from Bruker (Bruker Corporation, Billerica, MA, USA) in the wavelength range of 4000–300 cm^{-1} with an average of 16 scans and a resolution of 4 cm^{-1} in the absorbance mode. All the FTIR spectra were recorded at room temperature.

2.3.2. Differential scanning photo-calorimetry (photo-DSC)

A photocuring process of the initial solutions of sample A and sample A-P-AVI0.8-UV0h was studied by photo-DSC. Isothermal photo-DSC experiments were run under nitrogen flow (100 mL/min) with a Mettler Toledo (Greifensee, Switzerland) DSC-822e instrument. A Hamamatsu Lightningcure LC5 (Hg—Xe lamp) (Hamamatsu Photonics K. K., 325-6, Sunayama-cho, Naka-ku, Hamamatsu City, Shizuoka, 430-8587, Japan) with one beam conveniently adapted to the DSC was used to irradiate the investigated samples. The irradiation intensity was 17 mW/cm^2 (measured at 365 nm). The temperature was 25 °C during a total time of 8 min. The samples were analyzed with standard aluminum crucibles using a mass of approximately 5 mg. The equipment was previously calibrated with indium (156.6 °C) and zinc (419.6 °C) pearls.

2.3.3. Elemental organic analysis

Elemental analysis was used to determine Carbon, Hydrogen and Nitrogen content of the following 3 samples: A; A-PM-UV0h and A-PM-UV24h (i.e., without any core material), by means of Perkin Elmer EA2400 Elemental Analyzer (Perkin Elmer, Waltham, MA, USA). Tests were performed in duplicate and the amount of analyzed capsules was approximately 3 mg.

2.3.4. Inductively coupled plasma optical emission spectrometry (ICP-OES)

Calcium and sodium contents in samples A; A-PM-UV0h and A-PM-UV24h were determined using an ICP-OES Agilent 5100 analyzer (Agilent Technology, Santa Clara, CA, USA). The samples were analyzed in duplicate, after digestion overnight in HNO_3 or HCl. Around 2–3 mg of each sample were used for each analysis. Calcium and sodium concentrations were determined from the absorption intensities (Ca: 422.7 nm; Na: 589.6 nm) by interpolation of the calibration curves of intensity vs. concentration (ppm).

2.3.5. Optical microscopy (OM)

The prepared macrocapsules were observed with a Digital Microscope Leica DMS1000 (Wetzlar, Germany). The ImageJ (version 1.52, publicly available from the National Institutes of Health, Bethesda, MD, USA; http://imagej.nih.gov/ij/) software was used to measure the diameter of the capsules of each analyzed sample. (The diameter of between 15 and 20 capsules of each sample was measured before calculating the average value and its corresponding sampling error as shown in Table 2).

2.3.6. Environmental scanning electron microscopy (ESEM)

ESEM analysis were performed using a FEI Quanta 200 FEG (Hillsboro, OR, USA) in high vacuum mode, using a secondary electron detector and an accelerating voltage of 20 kV. Both the outer surface and the cross-section of the capsules were analyzed. Before the analysis, samples were coated on a tape surface with gold by means of a quorum Q150TS Plus sputter coater. To observe the cross-section, Leica CM 1950 Cryostat (Wetzlar, Germany) was used. The sample was mixed with an embedding medium (OCT Compound) and frozen at −25 °C on an aluminum support inside the machine. Once frozen, the sample was cut into slices of thickness 20 μm which were deposited on a microscopic slide.

2.3.7. Field emission scanning electron microscopy (FESEM)

Selected capsules were analyzed using a FESEM-FIB Scios 2 from FEI Company (Hillsboro, OR, USA) in high vacuum mode. In the same way as in the ESEM analysis, Leica CM 1950 Cryostat (Wetzlar, Germany) was used to observe the cross-section. The sample was mixed with an embedding medium (OCT Compound) and frozen at −25 °C on an aluminum support inside the machine. Once frozen, the sample is cut into slices of thickness 20 μm which were deposited on a microscopic slide. Prior to analysis, the slides were coated with carbon to avoid sample deterioration due to the high vacuum applied. The Energy Dispersive X-ray Spectroscopy (EDX) was used for analyzing the elemental composition of the capsules.

2.3.8. Dynamic mechanical analysis (DMA)

Dynamic mechanical analysis was carried out using a DMA Q800 V21.3 Build 96 from TA instruments (New Castle, DE, USA) working on a controlled compression force on the capsule samples. Capsules from samples A-AVI0.8; A-PM-AVI0.8-UV0h and A-PM-AVI0.8-UV24h were examined. The number of tested capsules ranged between 7 and 9.

The temperature, the position of the probe, the force applied, the stress, the strain, the stiffness, the creep compliance and the relaxation modulus of each type of capsules were recorded with respect to the time until the rupture occurs. Besides, the maximum force obtained for each type of capsule was also recorded. On the other hand, the stiffness value was obtained for each capsule by taking the slope of the linear part of the force variation as a function of length.

2.3.9. Thermogravimetric analysis (TGA)

Thermal stability studies of the capsules were carried out in ALU OXIDE crucibles of 70 μL (ME-24123) with a Mettler Toledo TGA2 thermobalance (Mettler Toledo, Columbus, OH, USA). Samples A; A-AVI0.8; A-PM-UV0h; A-PM-AVI0.8-UV0h; A-PM-UV24h and A-PM-AVI0.8-UV24h, weighing around 6–8 mg, were heated between 30 and 600 °C at a heating rate of 10 °C/min in N_2 atmosphere with a flow rate of 50 cm^3/min. The equipment was previously calibrated with indium (156.6 °C) and aluminum (660.3 °C) pearls.

2.3.10. Total organic carbon (TOC)

TOC is the amount of carbon found in an organic compound, which comes from oxidizing all organic matter present in water. It is commonly used to indicate the level of pollution in wastewater caused by organic compounds.

Basically, the TOC measurement is performed by converting all the kind of carbon from the sample into CO_2. There are direct and also indirect methods to carry out these measurements. The direct method was selected in our case.

In this method, the organic carbon (OC) was measured using the following steps:

(i) First of all, the inorganic carbon (IC) was removed through an acid treatment. Moreover, sample aeration prior to analysis eliminated errors due to the presence of inorganic carbon.
(ii) In the second step, the OC content (or non-purgeable organic carbon (NPOC) was determined by a chemical oxidation. The organic carbon of the sample was converted into CO_2 in a high temperature furnace. Finally, the CO_2 produced during the oxidation was measured by means of an FTIR detector.

In this way, TOC was quantitatively determined by interpolating the obtained values for each sample in the calibration curve prepared using potassium hydrogen phthalate (Sigma Aldrich, Burlington, MA, USA) as standard.

In this way, TOC analyses of the soluble fractions of samples A; A-PM-UV0h and A-PM-UV24h were carried out. To perform these analyses, first the water-soluble fraction of the capsules was obtained by this procedure: 500 mg of the capsules were crushed through a coffee

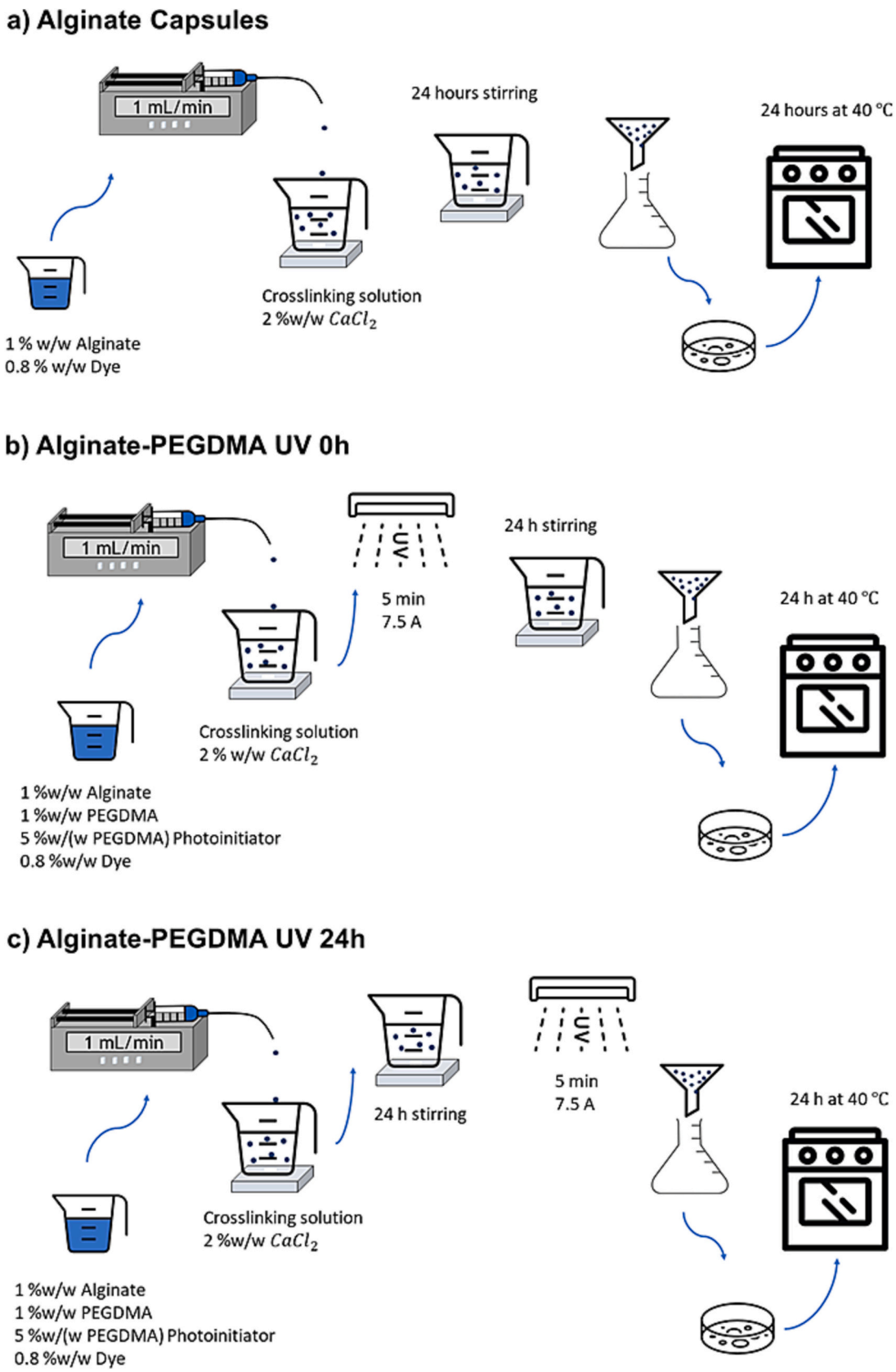

Fig. 2. Composition of the capsules and methodology followed in the dye encapsulation process of: a) capsules which shell is only made of alginate; b) Capsules which shell contains both alginate and PEGDMA and were irradiated with UV light before leaving them for 24 h under magnetic stirring; c) Capsules which shell contains both alginate and PEGDMA and were irradiated with UV light after leaving them for 24 h under magnetic stirring.

Table 2
Elemental composition determined by elemental organic analysis and ICP-OES (%).

Sample	Weight (%)				
	C	H	N	Ca	Na
A	15.7 ± 0.2	4.72 ± 0.09	0.18 ± 0.01	12.3 ± 0.3	0.56 ± 0.01
A-PM-UV0h	18.6 ± 0.3	4.92 ± 0.01	0.23 ± 0.01	11.80[a]	0.52[a]
A-PM-UV24h	18.4 ± 0.3	4.77 ± 0.01	0.25 ± 0.02	12.0 ± 0.3	0.58 ± 0.02

[a] Only one sample could be analyzed by ICP-OES.

grinding machine (MKM6003, BOSCH, Gerlingen, Germany) for 30 s. Then, the crushed samples were added to 50 mL of milliQ water and left under stirring for 24 h. At this time, the solution was filtered, and the remaining capsules were dried and weighed. The filtered solutions were analyzed using a Total Organic Carbon analyzer TOC-L CSN 638-91109-48 equipment (Shimadzu Corporation, Kyoto, Japan). TOC analysis was repeated 3 times for each sample.

Moreover, the stability of the capsules at different pH was studied following the procedure described below:

First of all, 200 mg of empty capsules (samples A; A-PM-UV0h; and A-PM-UV24h) were crushed using a coffee grinding machine (MKM6003, BOSCH, Gerlingen, Germany) for 30 s. Then they were added to 20 mL of the Alkaline buffer solution. The obtained mixtures were left under stirring for 7 days at room temperature after which the remaining capsules were filtered, dried, and weighed to calculate the soluble part.

In another experiment, capsules A-PM-UV0h and A-PM-AVI0.8-UV0h were selected to evaluate their stability in acid (0.1 M HCl solution, pH = 1.0) and basic pH (0.1 M NaOH solution, pH = 13.0). The stability of both samples was evaluated following the same procedure described above with the Alkaline buffer solution.

3. Results and discussion

3.1. Preparation of the macrocapsules

As previously outlined, distinct factors of the polymerization should be controlled to favor the formation of multicomponent shell capsules. The first one involves the selection of a dye that has to be soluble in water in the desired concentration. In this study, 3 different dyes were tested: Reactive Orange 16, Auramine O and Active Violet Ion (AVI). From all of them, Reactive Orange 16 showed the highest solubility in water (>1 %). However, the release of this dye from the capsules is directly detected when the capsules are still forming in the calcium chloride solution. Even if a smaller amount of dye was used (samples A-RO0.1; A-RO0.3; A-RO0.5, Table 1), the same phenomenon was observed, which does not allow an appropriate encapsulation of the dye into the alginate-based shell because this system is not able to keep the dye within its structure during that time. In the case of Auramine O dye, its low solubility in water limits the quantity of encapsulated dye to a maximum value of 0.03 %. Even so, the liberation of Auramine O dye from alginate systems occurs as was also observed before for Reactive Orange 16 dye. On the other hand, AVI showed a solubility in water up to 0.8 %. In contrast with the two previously tested dyes, AVI was stable inside the alginate capsules at least for 24 h at different concentrations ranging from 0.1 to 0.8 % when it was tested. Therefore, the highest concentration at which AVI was stable was established as the optimal concentration of encapsulated dye (0.8 %) and was used for the preparation of the upcoming capsules.

The second analyzed point comprises the choice of the most appropriate acrylate derived from poly(ethylene glycol) that was used in the construction of the additional shell of the polymeric capsules. In this work, two acrylate monomers were tested: poly(ethylene glycol) diacrylate (PEGDA) and poly(ethylene glycol) dimethacrylate (PEGDMA), which can easily polymerize when the aqueous solution was irradiated with UV light.

However, when forming the capsules following the process described in Fig. 2, it was observed that the polymerization of the diacrylate monomer took place in a different phase from that in which the alginate is found depending on whether PEGDA or PEGDMA was used. Thus, alginate composite capsules were obtained in the latter case due to the good solubility in water of both alginate and PEGDMA. On the contrary, the formation of a second phase in the crosslinking solution occurred when the capsules were prepared with PEGDA because this monomer is not soluble in water and thus polymerized alone outside the water phase. Even so, capsule-shaped structures were obtained as observed by optical microscopy although PEGDA was not incorporated in them (Table S1). In fact, the observation of a white solid in addition to the water solution containing the alginate derived capsules confirmed the crosslinking of PEGDA in a separated phase [26].

Therefore, PEGDMA was selected as the acrylate monomer derived from poly(ethylene glycol) because its better solubility in water permits the formation of multicomponent shell capsules in a controlled manner.

3.2. Characterization of the macrocapsules

Once the composition of the solutions that enable the formation of macrocapsules with two components in their shell was well established, the synthesized capsules were characterized using different techniques to determine their properties.

3.2.1. Chemical characterization

The chemical characterization of the prepared systems was performed by FTIR, elemental organic analysis and ICP-OES.

First of all, FTIR analysis allowed us to monitor the chemical reactions that took place during the formation of the capsules:

1) The crosslinking of alginate by calcium ions.
2) The radical polymerization of PEGDMA.

The FTIR spectra of PEGDMA, sodium alginate and samples A; A-PM-UV0h and A-PM-UV24h are shown in Fig. 3. To understand what happens during the crosslinking of alginate induced by calcium ions, the FTIR spectra of sodium alginate and sample A must be compared. As observed in Fig. 3, different characteristic bands were observed in the FTIR of sodium alginate: a broad band centered at about 3260 cm^{-1}, which is attributed to the ν(O—H) stretching, two bands at 1600 and 1407 cm^{-1}, which correspond to the $\nu(COO^{-})$ symmetric and asymmetric stretching, respectively and a band at 1029 cm^{-1} attributed to the ν(C-O-C) stretching [27]. When the capsules were formed, the vast majority of sodium cations were replaced by calcium cations. Both ions present different ionic radius, charge density and atomic weight, which are related with the shift of the band associated to the asymmetric stretching of the carboxylate group and the decrease of the intensity of the band attributed to the ν(C-O-C) stretching [28,29]. Furthermore, the band related to the hydroxyl stretching becomes narrower and of higher intensity, indicating an increase in intramolecular bonding when alginate is crosslinked with Ca^{2+} [30].

Regarding the polymerization of PEGDMA, its FTIR spectra was compared with the spectra of the capsules formed after UV irradiation (samples A-PM-UV0h and A-PM-UV24h). In this case, a decrease of the bands at 819 cm^{-1} (δ(C=C) twisting) and 954 cm^{-1} (δ(C=C) bending), which are characteristic of the methacrylate functional group, confirmed that the polymerization of PEGDMA occurred [31–34]. Nevertheless, the observation of a small band at 819 cm^{-1} at the end of the curing process indicates that not all the methacrylate units of PEGDMA have been polymerized: actually, the reactivity of PEGDMA decreases during its polymerization since the resulting radicals become

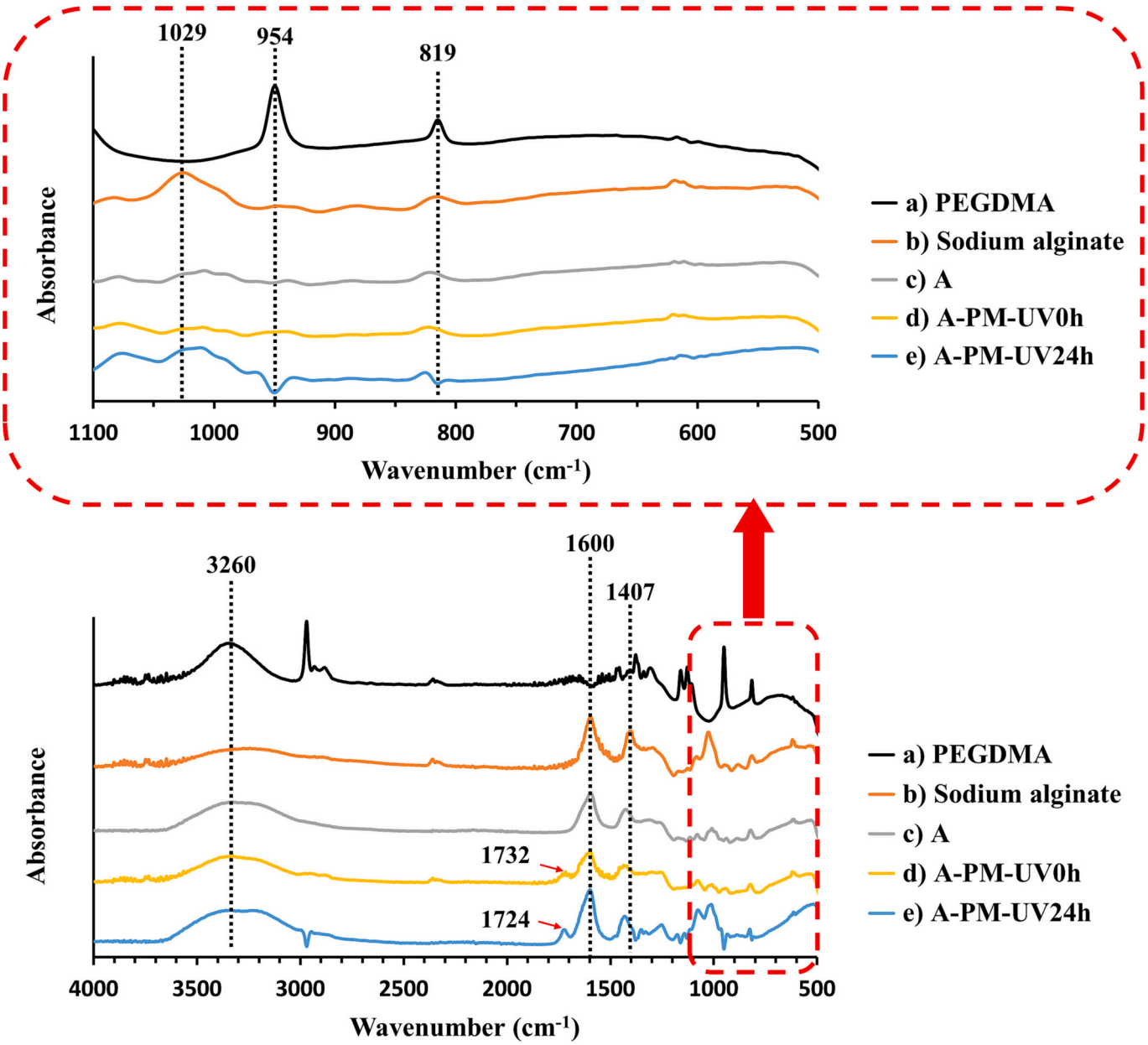

Fig. 3. FTIR spectra of: a) PEGDMA; b) Sodium alginate; c) A; d) A-PM-UV0h; e) A-PM-UV24h.

increasingly hindered [35]. Moreover, a band that is attributed to the ν(C=O) stretching of diacrylate groups is observed in the resulting interpenetrating networks of samples A-PM-UV0h (ν(C=O) = 1732 cm^{-1}) and A-PM-UV24h (ν(C=O) = 1724 cm^{-1}), demonstrating that PEGDMA has polymerized and been incorporated into the final network (Fig. 3) [36]. Additionally, the exothermal peak observed when an isothermal photo-DSC was carried out at room temperature of the initial mixture of sample A-P-AVI0.8-UV0h (without the AVI dye) before being photocured confirms that the diacrylic monomer has been polymerized (Fig. S1).

On the other hand, no significant differences were found in the FTIR spectra of the capsules that only differed by the presence or not of the encapsulated dye as observed in Fig. S2. According to Alshamrani and co-workers, it confirms the effective encapsulation of the dye inside the core of the macrocapsules [37].

The determination of the elemental composition in the case of the samples without the encapsulated dye (samples A; A-PM-UV0h and A-PM-UV24h) confirmed that sodium cations present in the used sodium alginate were mainly replaced by calcium cations during the cross-linking process (Table 2). As expected, the addition of PEGDMA increases the carbon content of the capsules. Furthermore, it was expected that the capsules whose shell was constituted only by alginate would present a greater amount of calcium cation because it is assumed that the incorporation of the diacrylate monomer could reduce the crosslinking capacity of Ca^{2+} with alginate. Nevertheless, no significant differences in Ca^{2+} content were detected between the 3 analyzed samples as shown in Table 2.

3.2.2. Morphological characterization

By optical microscopy, the first noticeable thing is that the capsules of all the samples (whether they content the dye or not) exhibited a spherical and regular shape as observed in Fig. 4a. Moreover, the average diameter of all the samples prepared are between 0.6 and 0.8 mm (Table S1). Another remarkable aspect is that the encapsulation of the dye in this system does not cause the obtained capsules to be larger than the ones that do not contain the dye. Besides, the diameter of the

capsules does not undergo considerable changes when the amount of encapsulated AVI was increased [38,39]. As regards capsules which shell also contains PEGDMA, its addition did not significantly affect their diameter, although capsules with a larger diameter would be expected [40]. In our case, the average diameter of all the capsules is mainly determined by the diameter of the syringe needle as stated by McClements [41].

The morphology of the resulting capsules was analyzed by ESEM (Fig. 4b and Fig. S3). From the figures, it can be noted that the capsules prepared only with sodium alginate without any encapsulated dye have the smoother surface (sample A in Fig. S3). The combination of both sodium alginate and PEGDMA confers a certain irregularity to the surface of the capsules compared to sample A. Furthermore, it is expected that the presence of the encapsulated AVI affects the morphology of the resulting capsules, causing its surface to be rougher. In fact, this was proved by the roughest surface of the capsules containing the encapsulated dye (samples A-AVI0.8; A-PM-AVI0.8-UV0h and A-PM-AVI0.8-UV24h), compared to that of the empty capsules (samples A; A-PM-UV0h and A-PM-UV24h).

This change in the morphology upon the incorporation of the dye in the capsules is probably due to the interaction between the dye and the alginate chains disturbing their crosslinking and leading to a less organized network [42,43].

In point of fact, the observed striae on the surface of the capsules from sample A-AVI0.8 are produced by the encapsulated AVI [44,45]. Moreover, it was shown that the preparation of the same capsules but irradiating them for 5 min with UV light makes their surface less rough (sample A-AVI0.8-UV0h in Fig. S3). Furthermore, the comparison of the surface of the capsules made up with both PEGDMA and sodium alginate with the entrapped dye (samples A-PM-AVI0.8-UV0h and A-PM-AVI0.8-UV24h) with the capsules of sample A-AVI0.8 proved that the UV light exposure leads to a smoother and more homogeneous surface.

Regarding sample A-PM-UV24h, a considerable number of pores was detected in the capsules cross-section. During the formation of these capsules, it is expected that the crosslinking of the alginate chains occurs before PEGDMA, since the polymerization of the diacrylate monomer was not favored until 24 h after its addition into the crosslinking solution. Therefore, alginate initially crosslinks and would establish the positions where PEGDMA crosslinking is going to take place, giving rise to a highly porous structure. In fact, this is confirmed by the presence of some pores in the capsules' cross-section of sample A-PM-AVI0.8-UV24h, although their number is much smaller since most of them would have been occupied by AVI.

Another parameter that affects the shape of the macrocapsules is the selected irradiation time of the water solution. As mentioned before, two different irradiation times were selected in this work:

1) Time 0 h, which means that the samples were irradiated directly after being extruded into the crosslinking solution of calcium chloride during 5 min (samples A-PM-UV0h and A-PM-AVI0.8-UV0h).
2) Time 24 h: the samples were irradiated during 5 min after being stirred for 24 h (samples A-PM-UV24h and A-PM-AVI0.8-UV24h).

From ESEM pictures of the cross-section, it can be evidenced that the latest irradiation of the crosslinking solution induces the formation of a more uniform and homogeneous network because Ca^{2+} and the dye can be better distributed in the capsule in addition to allow calcium cations to be more tightly coordinated with the alginate chains (samples A-PM-UV24h and A-PM-AVI0.8-UV24h).

On the other hand, the hollow spheres observed in the capsules cross-section of sample A-PM-AVI0.8-UV0h, where the dye is expected to be encapsulated inside the empty core, confirmed the hypothesis that PEGDMA crosslinks after its irradiation without allowing AVI or the calcium ions to diffuse across the capsule shell.

The distribution of the Ca^{2+} ions in the capsules irradiated at different times with encapsulated AVI dye (sample A-PM-AVI0.8-UV0h and A-PM-AVI0.8-UV24h) was checked by FESEM. As observed in Fig. 4c, the intensity of the yellow circles both in the center and on the edge of the capsules clearly showed that the location of calcium ions differs between the two investigated samples. On one side, calcium was distributed mainly inside the capsules on the boundaries of the holes in sample A-PM-AVI0.8-UV0h (Fig. 4c). On the other hand, a higher concentration of Ca^{2+} was found on the boundary of the capsules irradiated after 24 h under stirring (sample A-PM-AVI0.8-UV24h in Fig. 4c), which confirms the more uniform structure of the capsules irradiated after being stirred for 24 h in the crosslinking solution.

3.2.3. Mechanical properties

The mechanical properties of the capsules that contains the encapsulated AVI were evaluated by performing dynamic mechanical analysis (samples A-AVI0.8; A-PM-AVI0.8-UV0h and A-PM-AVI0.8-UV24h). So, the maximum stress, the maximum strain, the normalized average maximum force and the stiffness of each sample are summarized in Table 3. When the values of the three tested samples are compared, it is easily found that the capsules from sample A-AVI0.8, which contains only the alginate and the dye, are more resistant and stiffer than the capsules from samples A-PM-AVI0.8-UV0h and A-PM-AVI0.8-UV24h. These results are in accordance with literature, and evidence the more rigid character of alginate, whilst the presence of PEG based monomers provides greater flexibility to the shell of the capsules [46,47]. However, despite a different structure and morphology between the capsules of sample A-PM-AVI0.8-UV0h and A-PM-AVI0.8-UV24h was observed, it seems that the difference in the time of irradiation (instantaneous or after 24 h stirring, respectively) did not substantially affect the average value of the mechanical properties of the resulting capsules. Despite this, the higher standard deviations obtained for the capsules of sample A-PM-AVI0.8-UV0h confirmed that they are composed by a more heterogeneous structure than capsules of sample A-PM-AVI0.8-UV24h, as previously observed in the ESEM images. In accordance with our results, the alginate hydrogels reported by Kuo et al. showed a uniform distribution of calcium ions, resulting in homogenous hydrogels that exhibited a small standard deviation of their mechanical properties [48].

Furthermore, the examination of the physical structure of the broken capsules by optical microscopy demonstrated that they could experiment two distinct rupture mechanisms (Fig. 5):

- A fracture or a crack, which is experienced by the capsules from samples A-AVI0.8 and A-PM-AVI0.8-UV24h.
- An exfoliation or a peeling behavior, which is suffered by the capsules from sample A-PM-AVI0.8-UV0h.

The fact that the capsules can break down following one of the two mechanisms is closely related to their morphology and homogeneity of their structure, as observed in the standard deviation of the mechanical properties listed in Table 3. Thus, the multi-layer cross-section of heterogeneous capsules is expected to be broken down by an exfoliation in form of peeling the outer layer as observed in the capsules of sample A-PM-AVI0.8-UV0h. Instead, the other two types of capsules undergo crushing due to their more homogeneous cross-section.

3.2.4. Thermal properties

The TGA and DTGA curves of the samples without and with the encapsulated dye are shown in Figs. S4 and S5, respectively. As observed in the DGTA curves, the thermal degradation of these capsules showed mainly a three-step weight loss. The first mass loss was observed between 43 and 179 °C and is associated to the loss of water, which indicates that alginate capsules have a great tendency to absorb water (13–17 %) [49]. After that, the second and the third steps comprise the range between 179 and 258 °C and from 258 to 334 °C, respectively. Within these intervals, the decomposition of the alginate matrix occurred by different chemical processes: glycoside bond breaking, dehydration, decarboxylation and decarbonylation [50–52]. On the

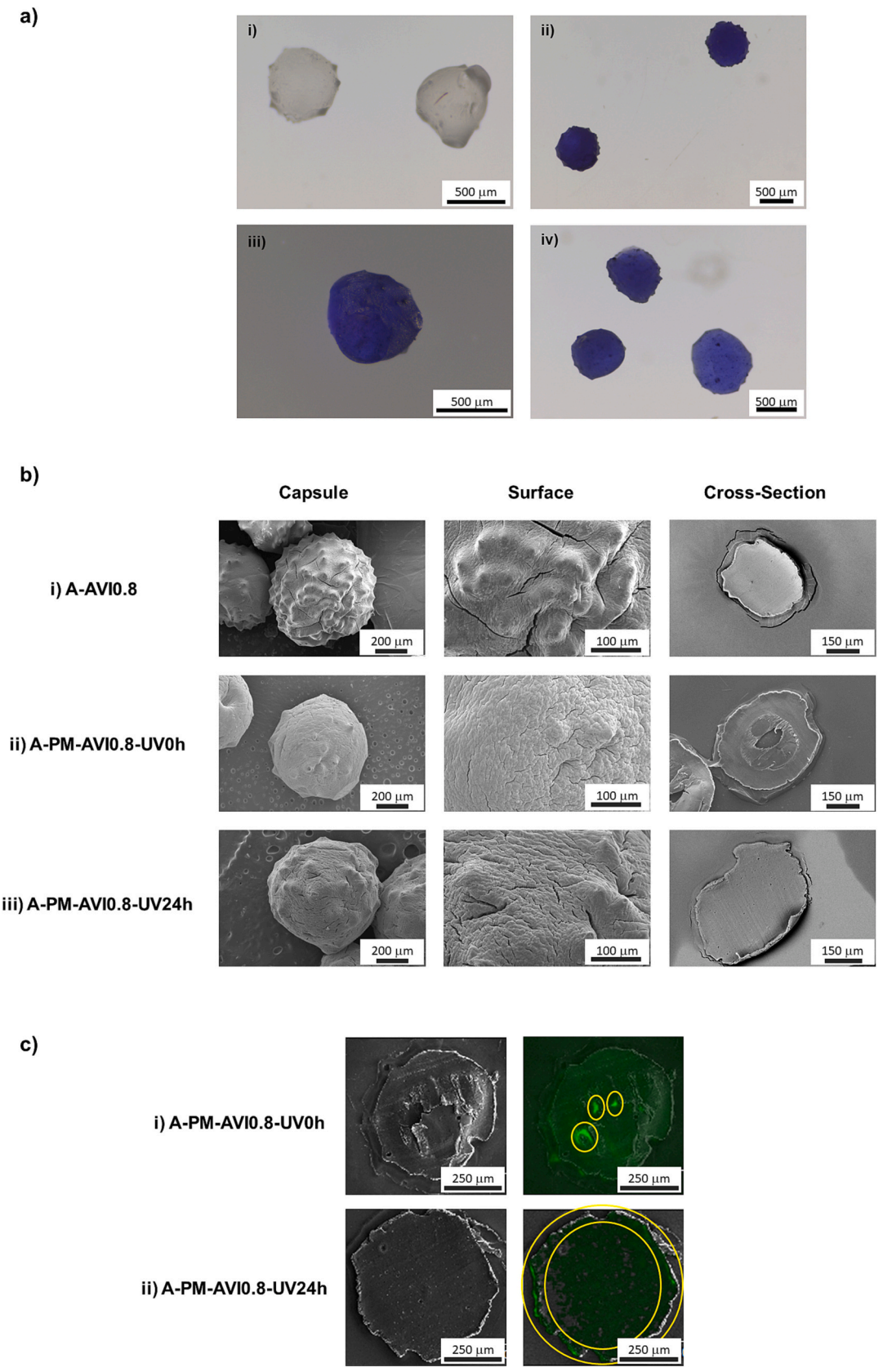

Fig. 4. a) Optical microscope images of capsules of the following samples: i) A, ii) A-AVI0.8, iii) A-PM-AVI0.8-UV0h and iv) A-PM-AVI0.8-UV24h; b) ESEM images of synthesized capsules showing the whole capsule (magnification x160), its surface (magnification x500) and its cross-section (magnification x209, x210, and x249 for A-AVI0.8, A-PM-AVI0.8-UV0h, and A-PM-AVI0.8-UV24h, respectively): i) A-AVI0.8, ii) A-PM-AVI0.8-UV0h and iii) A-PM-AVI0.8-UV24h; c) FESEM images and map (magnification x400) showing the distribution of Ca^{2+} ions in the capsules of: i) A-PM-AVI0.8-UV0h and ii) A-PM-AVI0.8-UV24h (regions highlighted in yellow indicate high concentration of calcium cations).

Table 3
Average maximum force and stiffness of the capsules.

Sample	Maximum Stress (MPa)	Maximum strain (%)	Normalized average maximum force[a] (N/mm)	Stiffness (N/mm)
A-AVI0.8	21 ± 6	−35 ± 7	19.55 ± 4.30	(54 ± 18) × 10^{-3}
A-PM-AVI0.8-UV0h	16 ± 5	−32 ± 9	15.44 ± 8.32	(39 ± 26) × 10^{-3}
A-PM-AVI0.8-UV24h	15 ± 3	−39 ± 4	15.9 ± 4.5	(34 ± 6) × 10^{-3}

[a] normalized to the initial sample length.

other hand, the presence of polyethylene glycol network is evident in samples A-PM-UV0h, A-PM-UV24h, A-PM-AVI0.8-UV0h and A-PM-AVI0.8-UV24h because an additional degradation step was detected in their DTGA curves between 334 and 371 °C [53]. Besides, the encapsulation of AVI did not substantially modify the TGA curves of the analyzed capsules as can be verified by comparing Figs. S4b and S5b. As a matter of fact, the analysis of the thermal stability of the dye alone showed only a one-step weight loss with a maximum centered at 141 °C and no char yield was detected at temperatures above 370 °C.

On the other hand, Table 4 collects the onset of 5 % mass loss and the char yield of the investigated samples, which allowed the assessment of the thermal stability and degradation profile of each type of capsules. Onset of thermal weight loss (temperature corresponding to 5 % mass loss) was between 91 and 95 °C for the capsules which shell is formed only by alginate. It is observed that the addition of polyethylene glycol network increases around 10 °C their onset of thermal weight loss of the resulting capsules without encapsulated AVI dye (samples A-PM-UV0h and A-PM-UV24h). Nonetheless, the samples that have incorporated the dye exhibited a slightly lower thermal stability compared with the empty ones, probably due to the interactions between the blue dye with alginate during the formation of the capsules, which would reduce its crosslinking capacity with calcium.

3.2.5. *Biodegradability studies*

Before approaching the study of the release of the AVI dye, we tackled the biodegradability of these capsules. Since it is expected to use them in laundry applications, the solvent used was water. So, the dissolved fraction in water of the capsules of samples A, A-PM-UV0h, and A-PM-UV24h is shown in Table 5.

The solubility of the alginate-based capsules (sample A) in water is determined by the solubility of the crosslinked alginate, for which a low water solubility is expected [54].

When the values of the systems under investigation are compared, it can be figured out that the addition of the polyethylene glycol network did not result in a decrease in the solubility of the capsules as would be expected [55] since samples A and A-PM-UV24h show a very similar water solubility. Nonetheless, the time at which the crosslinking solution that contains PEGDMA was irradiated induces meaningful differences in the water solubility of the obtained capsules. In fact, the capsules that were irradiated at time zero (sample A-PM-UV0h) had a higher solubility in water because the rapid polymerization of PEGDMA could initially limit the ability of crosslinking of alginate with calcium cations in the resulting composite structure [56]. Consequently, a less homogeneous network was formed that showed a higher solubility in water due to a greater interaction between crosslinked alginate and water. On the other hand, when the crosslinking of PEGDMA was not favored until 24 h after carrying out the extrusion of the polymeric solution (sample A-PM-UV24h), crosslinked alginate and polyethylene glycol networks were more homogeneously distributed in the shell of the capsules, which results in the obtention of the lowest soluble capsules in water [57].

Furthermore, the comparison of the soluble amount of the three types of capsules showed that the more homogeneous the structure of the system, the lower the soluble fraction of the capsules in water. This trend, that was evidenced by ESEM images, also determined the mechanical properties and the rupture mechanism of the capsules.

Table 4
Thermogravimetric data of the analyzed samples.

Sample	$T_{5\%}$ (°C)[a]	Char yield (%)[b]
A	95	44.9
A-AVI0.8	91	44.3
A-PM-UV0h	105	42.3
A-PM-UV24h	105	42.6
A-PM-AVI0.8-UV0h	82	41.7
A-PM-AVI0.8-UV24h	92	43.6

[a] Temperature of 5 % weight loss.
[b] Char residue at 600 °C.

Table 5
Quantity of capsules dissolved in water (%) after 1 day and TOC results of capsules from: A, A-PM-UV0h, A-PM-UV24h.

Sample	Dissolved quantity of capsules in water after 1 day (wt%)	TOC (mg/L)
A	45.6 ± 0.8	30.5 ± 8.5
A-PM-UV0h	56.0 ± 2.2	282.4 ± 14.7
A-PM-UV24h	42.3 ± 1.0	271.3 ± 8.9

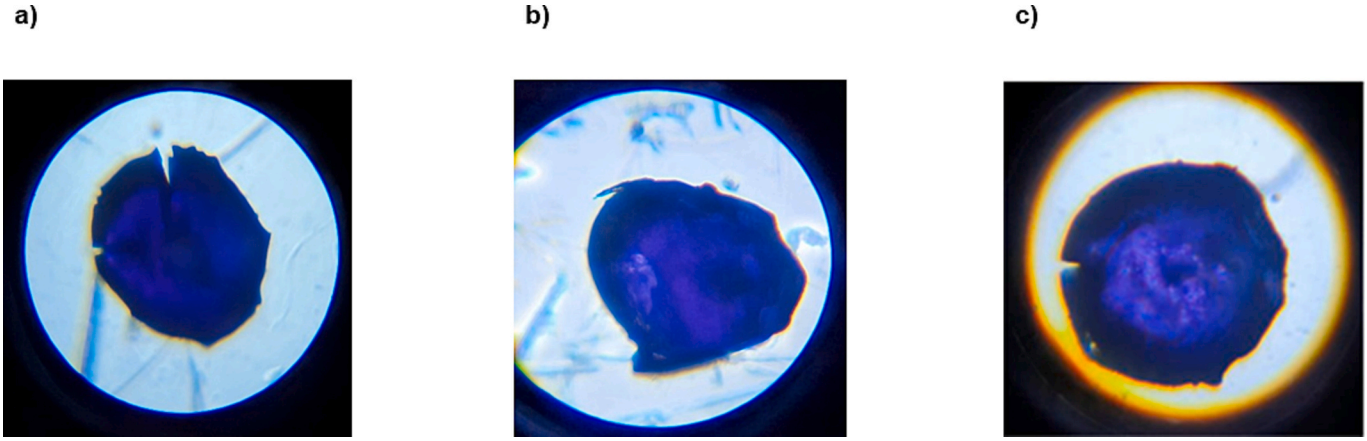

Fig. 5. Optical images of the capsules after rupture: a) A-AVI0.8; b) A-PM-AVI0.8-UV0h; c) A-PM-AVI0.8-UV24h.

Regarding the total organic content (TOC) of the soluble fractions in water, we observed that the soluble fractions of the alginate capsules clearly present a lower TOC value compared with the soluble fractions of the capsules which shell is constituted by both alginate and polyethylene glycol networks even though the mass of the soluble fractions that were recovered from each of the 3 samples was very similar. Moreover, the TOC of the soluble fractions of samples A-PM-UV0h and A-PM-UV24h were almost identical, although the TOC value is slightly higher for the sample that is more soluble in water.

On the other hand, the stability of the capsules was also evaluated at an acid and basic pH. First of all, the stability of the capsules of samples A; A-PM-UV0h and A-PM-UV24h was evaluated in the Alkaline buffer solution (pH = 10.3) to determine if there is any difference between the amount of soluble capsules in the solution of each type of capsules. This preliminary test evidenced that the 3 tested samples showed that a similar amount of the capsules was dissolved in the alkaline solution after 7 days as observed in Table S2. Then, capsules of the sample A-PM-UV0h and A-PM-AVI0.8-UV0h were chosen to study the stability in an acid medium (pH = 1.0) and in a basic medium (pH = 13.0).

Fig. S6 shows the different photos that have been taken at different time intervals of the solutions under investigation. When we compared them, it was clearly observed that the different pH affects the stability of the capsules added into the solutions. In fact, the turbidity of the solutions in basic media increased as the days go by, whether they have the encapsulated dye (A-PM-AVI0.8-UV0h) or are empty (A-PM-UV0h). Actually, the intensity of the solution colour also increased for the capsules that contains the dye, evidencing that the blue dye is released during the experiment. On the contrary, the acid solutions remained transparent throughout the experiment and no dye release was detected.

Another remarkable aspect that confirms the stability of the capsules in acid pH is that the capsules' structure is kept after 7 days, while there was no evidence of capsule structures at the end of the experiment performed in 0.1 M NaOH solution. These results are in accordance with literature since it is described that alginate capsules swell and release the encapsulated materials in an alkaline media while they shrink and are resistant in an acidic media [58,59].

4. Conclusions

The development of biobased capsules formed by alginate shell or by a mixture of alginate and polyethylene glycol network was successfully accomplished. Moreover, a blue dye was efficiently encapsulated in the three different types of prepared capsules.

It was observed that favoring the polymerization of the diacrylate monomer at different times also induces important changes in the chemical, morphological, mechanical, and thermal properties of the resulting capsules. In fact, the most homogeneous network was obtained when the capsules with the encapsulated blue dye were left 24 h inside the calcium chloride crosslinking solution before irradiation with UV light. More precisely, these capsules showed the highest thermal stability and the smallest soluble fraction in water after 24 h because the PEGDMA can diffuse more effectively and polymerize together with the crosslinked alginate structure after that time, resulting in a more homogeneous and better organized system. On the contrary, the capsules that were irradiated just after the extrusion exhibited an empty core and a heterogeneous structure.

As regards the mechanical properties, it is noteworthy that the capsules that do not contain the diacrylate monomer in the formulation exhibited higher stiffness compared to the capsules formed with both monomers. Moreover, we have proved that the composition of the capsules shell is associated to a different rupture process.

Overall, the obtained results suggest that these biobased capsules may be potential candidates for application in the encapsulation of organic bleaching agents in the laundry detergents sector, although a profound investigation is still required to determine how the blue dye will be released from the capsules.

Supplementary data to this article can be found online at https://doi.org/10.1016/j.ijbiomac.2023.123530.

CRediT authorship contribution statement

Yasmin Kabalan: Methodology and investigation, Formal analysis, Writing – original draft preparation. **Xavier Montané:** Conceptualization, Formal analysis, Data curation, Validation, Supervision, Writing – review & editing, Funding acquisition, Resources. **Bartosz Tylkowski:** Conceptualization, Formal analysis, Data curation, Validation, Supervision, Funding acquisition, Resources. **Silvia De la Flor:** Methodology and investigation, Formal analysis. **Marta Giamberini:** Conceptualization, Formal analysis, Data curation, Validation, Supervision, Writing – review & editing, Funding acquisition, Project administration, Resources.

Declaration of competing interest

The authors declare that they have no known competing financial interests or personal relationships that could have appeared to influence the work reported in this paper.

Acknowledgements

This work was supported by the Ministerio de Ciencia e Innovación, grant number PID2020-116322RB-C32. This project has received funding from the European Union's Horizon 2020 research and innovation programme under the Marie Skłodowska-Curie grant agreement No. 713679. The authors also acknowledge Dr. Rita Marimón Picó, Dr. Mariana Stefanova Stankova and Núria Argany Figueras for their help in ESEM and FESEM analysis (Scientific & Technical Resources Service, Universitat Rovira i Virgili), while also thanking Dr. Esther Torrens Serrahima (Research technician, Department of Chemical Engineering, Universitat Rovira i Virgili) for her help in TOC experiments.

References

[1] E. Bulut, Y. Turhan, Synthesis and characterization of temperature-sensitive microspheres based on acrylamide grafted hydroxypropyl cellulose and chitosan for the controlled release of amoxicillin trihydrate, Int. J. Biol. Macromol. 191 (2021) 1191–1203, https://doi.org/10.1016/j.ijbiomac.2021.09.193.

[2] J.M. Budinčić, L. Petrović, L. Đekić, J. Fraj, S. Bučko, J. Katona, L. Spasojević, Study of vitamin E microencapsulation and controlled release from chitosan/sodium lauryl ether sulfate microcapsules, Carbohydr. Polym. 251 (2021), 116988, https://doi.org/10.1016/j.carbpol.2020.116988.

[3] Y.M. Kim, K. Lee, Y. Lee, K. Yang, D. Choe, Y.H. Roh, Thermoresponsive semi-interpenetrating gelatin-alginate networks for encapsulation and controlled release of scent molecules, Int. J. Biol. Macromol. 208 (2022) 1096–1105, https://doi.org/10.1016/j.ijbiomac.2022.03.185.

[4] M. Shao, S. Li, C.P. Tan, S. Kraithong, Q. Gao, X. Fu, B. Zhang, Q. Huang, Encapsulation of caffeine into starch matrices: bitterness evaluation and suppression mechanism, Int. J. Biol. Macromol. 173 (2021) 118–127, https://doi.org/10.1016/j.ijbiomac.2021.01.043.

[5] Q. Zhang, D. Li, S. Guan, D. Liu, J. Wang, G. Xing, L. Yue, D. Cai, Tumor-targeted delivery of honokiol via polysialic acid modified zein nanoparticles prevents breast cancer progression and metastasis, Int. J. Biol. Macromol. 203 (2022) 280–291, https://doi.org/10.1016/j.ijbiomac.2022.01.148.

[6] B. Tylkowski, M. Olkiewicz, X. Montane, A. Nogalska, M. Haponska, J. M. Montornes, J. Kowalska, E. Malusá, Encapsulation technologies in agriculture, in: B. Tylkowski, M. Giamberini, S.F. Prieto (Eds.), Microencapsulation, 2nd Edition, De Gruyter, Berlin/Boston, 2020, pp. 287–302.

[7] Polaris Market Research, Laundry Detergent Market Share, Size, Trends, Industry Analysis Report, By Product; By Application; By Region; Segment Forecast, 2022 - 2029, 2021.

[8] E. Smulders, E. Sung, Laundry detergents, 2. Ingredients and products, in: Ullmann's Encyclopedia of Industrial Chemistry, Wiley-VCH, 2012, pp. 393–447.

[9] H. Salas, C. Gutiérrez-Bouzán, V. López-Grimau, M. Vilaseca, Respirometric study of optical brighteners in textile wastewater, Materials 12 (2019) 785, https://doi.org/10.3390/ma12050785.

[10] M. Soltanzadeh, S.H. Peighambardoust, B. Ghanbarzadeh, M. Mohammadi, J. M. Lorenzo, Chitosan nanoparticles encapsulating lemongrass (Cymbopogon commutatus) essential oil: physicochemical, structural, antimicrobial and in-vitro release properties, Int. J. Biol. Macromol. 192 (2021) 1084–1097, https://doi.org/10.1016/j.ijbiomac.2021.10.070.

[11] B. Peña, C. Panisello, G. Aresté, R. Garcia-Valls, T. Gumí, Preparation and characterization of polysulfone microcapsules for perfume release, Chem. Eng. J. 179 (2012) 394–403, https://doi.org/10.1016/j.cej.2011.10.090.
[12] C.S.N.R. Teixeira, I.M.D. Martins, V.L.G. Mata, M.F. Filipe Barreiro, A.E. Rodrigues, Characterization and evaluation of commercial fragrance microcapsules for textile application, J. Text. Inst. 103 (2012) 269–282, https://doi.org/10.1080/00405000.2011.566312.
[13] X. Fei, H. Zhao, B. Zhang, L. Cao, M. Yu, J. Zhou, L. Yu, Microencapsulation mechanism and size control of fragrance microcapsules with melamine resin shell, Colloids Surf. A Physicochem. Eng. Asp. 469 (2015) 300–306, https://doi.org/10.1016/j.colsurfa.2015.01.033.
[14] S. Bône, C. Vautrin, V. Barbesant, S. Truchon, I. Harrison, C. Geffroy, Microencapsulated fragrances in melamine formaldehyde resins, Chimia (Aarau) 65 (2011) 177–181, https://doi.org/10.2533/chimia.2011.177.
[15] D.S. Kang, N. Lee, D.Y. Shin, Y.J. Jang, S.H. Lee, K.M. Lim, Y.S. Ahn, C.M. Lee, Y. R. Seo, Network-based integrated analysis for toxic effects of high-concentration formaldehyde inhalation exposure through the toxicogenomic approach, Sci. Rep. 12 (2022) 5645, https://doi.org/10.1038/s41598-022-09673-0.
[16] C. Umansky, A.E. Morellato, M. Rieckher, M.A. Scheidegger, M.R. Martinefski, G. A. Fernández, O. Pak, K. Kolesnikova, H. Reingruber, M. Bollini, G.P. Crossan, N. Sommer, M.E. Monge, B. Schumacher, L.B. Pontel, Endogenous formaldehyde scavenges cellular glutathione resulting in redox disruption and cytotoxicity, Nat. Commun. 13 (2022) 745, https://doi.org/10.1038/s41467-022-28242-7.
[17] M. Hauptmann, J.H. Lubin, P.A. Stewart, R.B. Hayes, A. Blair, Mortality from solid cancers among workers in formaldehyde industries, Am. J. Epidemiol. 159 (2004) 1117–1130, https://doi.org/10.1093/aje/kwh174.
[18] K. Bruyninckx, M. Dusselier, Sustainable chemistry considerations for the encapsulation of volatile compounds in laundry-type applications, ACS Sustain. Chem. Eng. 7 (2019) 8041–8054, https://doi.org/10.1021/acssuschemeng.9b00677.
[19] J.A.Ivar Do Sul, M.F. Costa, The present and future of microplastic pollution in the marine environment, Environ. Pollut. 185 (2014) 352–364, https://doi.org/10.1016/j.envpol.2013.10.036.
[20] M.A. Browne, P. Crump, S.J. Niven, E. Teuten, A. Tonkin, T. Galloway, R. Thompson, Accumulation of microplastic on shorelines worldwide: sources and sinks, Environ. Sci. Technol. 45 (2011) 9175–9179, https://doi.org/10.1021/es201811s.
[21] L. Cao, W. Lu, A. Mata, K. Nishinari, Y. Fang, Egg-box model-based gelation of alginate and pectin: a review, Carbohydr. Polym. 242 (2020), 116389, https://doi.org/10.1016/j.carbpol.2020.116389.
[22] B. Reig-Vano, B. Tylkowski, X. Montané, M. Giamberini, Alginate-based hydrogels for cancer therapy and research, Int. J. Biol. Macromol. 170 (2021) 424–436, https://doi.org/10.1016/j.ijbiomac.2020.12.161.
[23] C. Hu, W. Lu, A. Mata, K. Nishinari, Y. Fang, Ions-induced gelation of alginate: mechanisms and applications, Int. J. Biol. Macromol. 177 (2021) 578–588, https://doi.org/10.1016/j.ijbiomac.2021.02.086.
[24] J. Zhu, Bioactive modification of poly(ethylene glycol) hydrogels for tissue engineering, Biomaterials 31 (2010) 4639–4656, https://doi.org/10.1016/j.biomaterials.2010.02.044.
[25] J.D. Clapper, J.M. Skeie, R.F. Mullins, C.A. Guymon, Development and characterization of photopolymerizable biodegradable materials from PEG-PLA-PEG block macromonomers, Polymer (Guildf) 48 (2007) 6554–6564, https://doi.org/10.1016/j.polymer.2007.08.023.
[26] C. Nam, J. Yoon, S.A. Ryu, C.H. Choi, H. Lee, Water and oil insoluble PEGDA-based microcapsule: biocompatible and multicomponent encapsulation, ACS Appl. Mater. Interfaces 10 (2018) 40366–40371, https://doi.org/10.1021/acsami.8b16876.
[27] M. Farno, C. Lamarche, C. Tenailleau, S. Cavalié, B. Duployer, D. Cussac, A. Parini, B. Sallerin, S. Girod Fullana, Low-energy electron beam sterilization of solid alginate and chitosan, and their polyelectrolyte complexes, Carbohydr. Polym. 261 (2021), 117578, https://doi.org/10.1016/j.carbpol.2020.117578.
[28] C. Larosa, M. Salerno, J.S. de Lima, R. Merijs Meri, M.F. da Silva, L.B. de Carvalho, A. Converti, Characterisation of bare and tannase-loaded calcium alginate beads by microscopic, thermogravimetric, FTIR and XRD analyses, Int. J. Biol. Macromol. 115 (2018) 900–906, https://doi.org/10.1016/j.ijbiomac.2018.04.138.
[29] G. Lawrie, I. Keen, B. Drew, A. Chandler-Temple, L. Rintoul, P. Fredericks, L. Grøndahl, Interactions between alginate and chitosan biopolymers characterized using FTIR and XPS, Biomacromolecules 8 (2007) 2533–2541, https://doi.org/10.1021/bm070014y.
[30] R.I. Castro, L. Morales-Quintana, N. Alvarado, L. Guzmán, O. Forero-Doria, F. Valenzuela-Riffo, V.F. Laurie, Design and optimization of a self-assembling complex based on microencapsulated calcium alginate and glutathione (Cag) using response surface methodology, Polymers (Basel) 13 (2021) 2080, https://doi.org/10.3390/polym13132080.
[31] X. Jiao, D. Zhao, Y. Zhang, Q. Wu, G. Qiu, X. Lu, X. Shi, Synthesis and studies of poly(ethylene glycol dimethacrylate) microcapsule, Colloid Polym. Sci. 294 (2016) 639–646, https://doi.org/10.1007/s00396-015-3815-1.
[32] I.H. Sajid, M.F.M. Sabri, S.M. Said, M.F.M. Salleh, N.N.N. Ghazali, R. Saidur, B. Subramaniam, S.W. Hasan, H.A. Jaffery, Crosslinked thermoelectric hydro-ionogels: a new class of highly conductive thermoelectric materials, Energy Convers. Manag. 198 (2019), 111813, https://doi.org/10.1016/j.enconman.2019.111813.
[33] H. Lin, E. van Wagner, J.S. Swinnea, B.D. Freeman, S.J. Pas, A.J. Hill, S. Kalakkunnath, D.S. Kalika, Transport and structural characteristics of crosslinked poly(ethylene oxide) rubbers, J. Membr. Sci. 276 (2006) 145–161, https://doi.org/10.1016/j.memsci.2005.09.040.
[34] T. Scherzer, Depth profiling of the conversion during the photopolymerization of acrylates using real-time FTIR-ATR spectroscopy, Vib. Spectrosc. 29 (2002) 139–145, https://doi.org/10.1016/S0924-2031(01)00202-8.
[35] G. Burke, Z. Cao, D.M. Devine, I. Major, Preparation of biodegradable polyethylene glycol dimethacrylate hydrogels via thiol-ene chemistry, Polymers (Basel) 11 (2019) 1339, https://doi.org/10.3390/polym11081339.
[36] R. Łyszczek, M. Gil, H. Głuchowska, B. Podkościelna, A. Lipke, P. Mergo, Hybrid materials based on PEGDMA matrix and europium(III) carboxylates -thermal and luminescent investigations, Eur. Polym. J. 106 (2018) 318–328, https://doi.org/10.1016/j.eurpolymj.2018.08.019.
[37] M. Alshamrani, N.J. Ayon, A. Alsalhi, O. Akinjole, Self-assembled nanomicellar formulation of docetaxel as a potential breast cancer chemotherapeutic system, Life. 12 (2022) 485, https://doi.org/10.3390/life12040485.
[38] B.B. Lee, R. Ibrahim, S.Y. Chu, N.A. Zulkifli, P. Ravindra, Alginate liquid core capsule formation using the simple extrusion dripping method, J. Polym. Eng. 35 (2015) 311–318, https://doi.org/10.1515/polyeng-2014-0174.
[39] S. Sakai, I. Hashimoto, K. Kawakami, Production of cell-enclosing hollow-core agarose microcapsules via jetting in water-immiscible liquid paraffin and formation of embryoid body-like spherical tissues from mouse ES cells enclosed within these microcapsules, Biotechnol. Bioeng. 99 (2008) 235–243, https://doi.org/10.1002/bit.21624.
[40] A. Kumar, S.S. Lahiri, H. Singh, Development of PEGDMA: MAA based hydrogel microparticles for oral insulin delivery, Int. J. Pharm. 323 (2006) 117–124, https://doi.org/10.1016/j.ijpharm.2006.05.050.
[41] D.J. McClements, Designing biopolymer microgels to encapsulate, protect and deliver bioactive components: physicochemical aspects, Adv. Colloid Interface Sci. 240 (2017) 31–59, https://doi.org/10.1016/j.cis.2016.12.005.
[42] S. Thakur, S. Pandey, O.A. Arotiba, Development of a sodium alginate-based organic/inorganic superabsorbent composite hydrogel for adsorption of methylene blue, Carbohydr. Polym. 153 (2016) 34–46, https://doi.org/10.1016/j.carbpol.2016.06.104.
[43] N. Belhouchat, H. Zaghouane-Boudiaf, C. Viseras, Removal of anionic and cationic dyes from aqueous solution with activated organo-bentonite/sodium alginate encapsulated beads, Appl. Clay Sci. 135 (2017) 9–15, https://doi.org/10.1016/j.clay.2016.08.031.
[44] L.S. Yakimova, E.G. Guralnik, D.N. Shurpik, V.G. Evtugyn, Y.N. Osin, E. A. Sokolova, I.I. Stoikov, E.V. Subakaeva, P.V. Zelenikhin, Morphology, structure and cytotoxicity of dye-loaded lipid nanoparticles based on monoamine pillar[5]arenes, Mater. Chem. Front. 4 (2020) 2962–2970, https://doi.org/10.1039/d0qm00547a.
[45] A.A. Goncharenko, I.A. Tarasyuk, Y.S. Marfin, K.V. Grzhegorzhevskii, A. R. Muslimov, A.B. Bondarenko, M.D. Lebedev, I.A. Kuz'min, A.S. Vashurin, K. V. Lepik, A.S. Timin, E.V. Rumyantsev, DDAO controlled synthesis of organo-modified silica nanoparticles with encapsulated fluorescent boron dipyrrins and study of their uptake by cancerous cells, Molecules 25 (2020) 3802, https://doi.org/10.3390/molecules25173802.
[46] P. Eiselt, K.Y. Lee, D.J. Mooney, Rigidity of two-component hydrogels prepared from alginate and poly(ethylene glycol)-diamines, Macromolecules 32 (1999) 5561–5566, https://doi.org/10.1021/ma990514m.
[47] W. Zhou, H. Zhang, Y. Liu, X. Zou, J. Shi, Y. Zhao, Y. Ye, Y. Yu, J. Guo, Sodium alginate-polyethylene glycol diacrylate based double network fiber: rheological properties of fiber forming solution with semi-interpenetrating network structure, Int. J. Biol. Macromol. 142 (2020) 535–544, https://doi.org/10.1016/j.ijbiomac.2019.09.125.
[48] C.K. Kuo, P.X. Ma, Ionically crosslinked alginate hydrogels as scaffolds for tissue engineering: Part 1. Structure, gelation rate and mechanical properties, Biomaterials 22 (2001) 511–521.
[49] Q. Wang, L. Zhang, Y. Liu, G. Zhang, P. Zhu, Characterization and functional assessment of alginate fibers prepared by metal-calcium ion complex coagulation bath, Carbohydr. Polym. 232 (2020), 115693, https://doi.org/10.1016/j.carbpol.2019.115693.
[50] Y. Liu, J.S. Wang, P. Zhu, J.C. Zhao, C.J. Zhang, Y. Guo, L. Cui, Thermal degradation properties of biobased iron alginate film, J. Anal. Appl. Pyrolysis 119 (2016) 87–96, https://doi.org/10.1016/j.jaap.2016.03.014.
[51] Y. Liu, X.R. Zhao, Y.L. Peng, D. Wang, L. Yang, H. Peng, P. Zhu, D.Y. Wang, Effect of reactive time on flame retardancy and thermal degradation behavior of bio-based zinc alginate film, Polym. Degrad. Stab. 127 (2016) 20–31, https://doi.org/10.1016/j.polymdegradstab. 2015.12.024.
[52] Y. Liu, C.J. Zhang, J.C. Zhao, Y. Guo, P. Zhu, D.Y. Wang, Bio-based barium alginate film: preparation, flame retardancy and thermal degradation behavior, Carbohydr. Polym. 139 (2016) 106–114, https://doi.org/10.1016/j.carbpol.2015.12.044.
[53] C.M. González-Henríquez, M.A. Sarabia-Vallejos, C.A. Terraza, Z.E. López-Cabaña, G.del C. Pizarro, In situ-preparation and characterization of silver-HEMA/PEGDA hydrogel matrix nanocomposites: Silver inclusion studies into hydrogel matrix, Arab. J. Chem. 12 (2019) 1413–1423, https://doi.org/10.1016/j.arabjc.2014.11.012.
[54] S. Roger, D. Talbot, A. Bee, Preparation and effect of Ca2+ on water solubility, particle release and swelling properties of magnetic alginate films, J. Magn. Magn. Mater. 305 (2006) 221–227, https://doi.org/10.1016/j.jmmm.2006.01.005.
[55] J.W. Hwang, S.M. Noh, B. Kim, H.W. Jung, Gelation and crosslinking characteristics of photopolymerized poly(ethylene glycol) hydrogels, J. Appl. Polym. Sci. 132 (2015) 41939, https://doi.org/10.1002/app.41939.
[56] J. Fan, Z. Shi, M. Lian, H. Li, J. Yin, Mechanically strong graphene oxide/sodium alginate/polyacrylamide nanocomposite hydrogel with improved dye adsorption capacity, J. Mater. Chem. A 1 (2013) 7433–7443, https://doi.org/10.1039/c3ta10639j.

[57] J. Sung, D.G. Lee, S. Lee, J. Park, H.W. Jung, Crosslinking dynamics and gelation characteristics of photo- and thermally polymerized poly(ethylene glycol) hydrogels, Materials. 13 (2020) 3277, https://doi.org/10.3390/MA13153277.
[58] M. Suhail, X.R. Li, J.Y. Liu, W.C. Hsieh, Y.W. Lin, P.C. Wu, Fabrication of alginate based microgels for drug-sustained release: in-vitro and in-vivo evaluation, Int. J. Biol. Macromol. 192 (2021) 958–966, https://doi.org/10.1016/j.ijbiomac.2021.10.054.
[59] E. Gunter, O. Popeyko, Delivery system for grape seed extract based on biodegradable pectin-zn-alginate gel particles, Int. J. Biol. Macromol. 219 (2022) 1021–1033, https://doi.org/10.1016/j.ijbiomac.2022.08.040.